This article was downloaded by: [Purdue University]
On: 13 February 2013, At: 14:10
Publisher: Taylor & Francis
Informa Ltd Registered in England and Wales Registered Number: 1072954 Registered office: Mortimer House, 37-41 Mortimer Street, London W1T 3JH, UK

Philosophical Magazine
Publication details, including instructions for authors and subscription information:
http://www.tandfonline.com/loi/tphm20

AFM and Raman studies of topological insulator materials subject to argon plasma etching

Isaac Childres [a b] , Jifa Tian [a b] , Ireneusz Miotkowski [a b] & Yong Chen [a b c]

[a] Department of Physics, Purdue University, West Lafayette, IN 47907, USA

[b] Birck Nanotechnology Center, Purdue University, West Lafayette, IN 47907, USA

[c] School of Electrical and Computer Engineering, Purdue University, West Lafayette, IN 47907, USA

Version of record first published: 26 Sep 2012.

To cite this article: Isaac Childres , Jifa Tian , Ireneusz Miotkowski & Yong Chen (2013): AFM and Raman studies of topological insulator materials subject to argon plasma etching, Philosophical Magazine, 93:6, 681-689

To link to this article: http://dx.doi.org/10.1080/14786435.2012.728009

PLEASE SCROLL DOWN FOR ARTICLE

Full terms and conditions of use: http://www.tandfonline.com/page/terms-and-conditions

This article may be used for research, teaching, and private study purposes. Any substantial or systematic reproduction, redistribution, reselling, loan, sub-licensing, systematic supply, or distribution in any form to anyone is expressly forbidden.

The publisher does not give any warranty express or implied or make any representation that the contents will be complete or accurate or up to date. The accuracy of any instructions, formulae, and drug doses should be independently verified with primary sources. The publisher shall not be liable for any loss, actions, claims, proceedings, demand, or costs or damages whatsoever or howsoever caused arising directly or indirectly in connection with or arising out of the use of this material.

Philosophical Magazine, 2013
Vol. 93, No. 6, 681–689, http://dx.doi.org/10.1080/14786435.2012.728009

Taylor & Francis
Taylor & Francis Group

AFM and Raman studies of topological insulator materials subject to argon plasma etching

Isaac Childres[ab]*, Jifa Tian[ab], Ireneusz Miotkowski[ab] and Yong Chen[abc]

[a]*Department of Physics, Purdue University, West Lafayette, IN 47907, USA;* [b]*Birck Nanotechnology Center, Purdue University, West Lafayette, IN 47907, USA;* [c]*School of Electrical and Computer Engineering, Purdue University, West Lafayette, IN 47907, USA*

(*Received 14 June 2012; final version received 3 September 2012*)

Plasma etching is an important tool in nano-device fabrication. We report a study on argon plasma etching of topological insulator materials Bi_2Se_3, Bi_2Te_3, Sb_2Te_3 and Bi_2Te_2Se using exfoliated flakes (with starting thicknesses of ~100 nm) derived from bulk crystals. We present data mainly from atomic force microscopy (AFM) and Raman spectroscopy. Through AFM measurements, plasma exposure is observed to decrease the thickness of our samples and increase surface roughness (with height fluctuations reaching as large as ~20 nm). We extract an etching rate for each type of material. Plasma exposure also causes a widening (especially E_g^2) of the characteristic Raman peaks, with no significant change in peak position. The overall Raman intensity is observed to initially increase then decrease sharply after the samples are etched below ~20 nm in thickness. Our findings are valuable for understanding the effects of argon plasma etching on topological insulator materials.

Keywords: topological insulator; bismuth selenide; bismuth telluride; plasma etching; Raman spectroscopy; atomic force microscopy

1. Introduction

Topological insulator (TI) materials have received much attention recently in the scientific community because of their distinct properties and potential in nano-electronic applications [1]. Topological insulators are three-dimensional materials that are insulating in the bulk, but conductive on the surface, creating a two-dimensional system with Dirac fermions. Some of the most common examples of TI materials are Bi_2Se_3, Bi_2Te_3, Bi_2Te_2Se [2] and Sb_2Te_3.

Argon plasma etching is a tool commonly used in conjunction with lithographic techniques to fabricate topological insulator thin films or flakes such as Bi_2Se_3 and Bi_2Te_3 into devices. Our goal here is to investigate what changes plasma etching will induce in topological insulator materials. This study is inspired by our previous study of oxygen plasma etching of graphene [3]. The oxygen plasma etching results in marked changes in the graphene, including the introduction of new defect-related

*Corresponding author. Email: ichildre@purdue.edu

© 2013 Taylor & Francis

Downloaded by [Purdue University] at 14:10 13 February 2013

Raman peaks (e.g. D and D′), pit formation in atomic force microscopy (AFM) profiles and significantly modified electronic transport properties (e.g. reduced conductivity and mobility as well as emergence of weak localization) [3]. We hope to investigate the effects of the similar defect-generation method on the Raman spectra and AFM profiles of TI materials.

Downloaded by [Purdue University] at 14:10 13 February 2013

2. Methodology

High quality bulk topological insulator crystals Bi_2Se_3, Bi_2Te_3, Sb_2Te_3 and Bi_2Te_2Se have been synthesized using the Bridgeman method [4]. Samples studied in this work were fabricated using micromechanical exfoliation of bulk crystals onto a 300 nm SiO_2/Si substrate. Once peeled, the samples were located using an optical microscope and then confirmed to be ~100 nm thick using AFM. Flakes with such thickness are desired so that they can be gradually etched away in a reasonable amount of argon plasma exposures in our study. Once topological insulator flakes were identified to be the proper thickness, they were then characterized further using AFM and Raman spectroscopy before and after various amounts of exposure to an argon plasma.

Our plasma etching was performed in a microwave plasma system (Plasma-Preen II-382) operating at 100 W. A constant flow of argon (3 sccm) is pumped through the sample space in rough vacuum (<40 Torr), and the gas is excited by microwaves (operating for 1 or 2 s at a time), generating an ionized argon plasma. The microwave-excited plasma pulses are applied to the samples cumulatively, and AFM and Raman measurements are performed in ambient atmosphere and temperature after each successive exposure.

AFM measurements were performed using an ambient AFM system (NT-MDT NTEGRA Probe NanoLaboratory) operating in the tapping mode, where an area of ~10 μm × 10 μm around a TI flake is scanned. The thickness quoted below is averaged from an interior area of the sample.

Raman measurements were performed using a confocal Raman microscope (Horiba XploRA) with a 532 nm excitation laser, averaging four acquisitions each of 20 s. The power of the laser is kept low (~200 μW) with a laser spot size of ~1 μm in diameter. We use Raman spectroscopy to study the E_g^2 and A_{1g}^2 crystal vibrational modes [5] in our topological insulator samples. We cannot observe the lower vibrational modes E_g^1 and A_{1g}^1 because they appear at wavenumbers inaccessible for the filter of our Raman detector.

3. Results and discussion

Figure 1a–c show selected AFM images of a Bi_2Se_3 flake after various amounts of plasma etching. Height profiles along the horizontal lines for various stages of the etching process are plotted in Figure 1d. As is the case of all the topological insulator flakes we studied, plasma etching reduces the height of the samples in a non-uniform manner across the whole flake. Initially, the flakes exhibit a relatively smooth surface. However, the surfaces become increasingly rough the longer they are plasma etched, reaching a roughness (height fluctuation) as large as ~20 nm. Additionally, some edges of a sample are etched at a much lower rate than the rest of the sample,

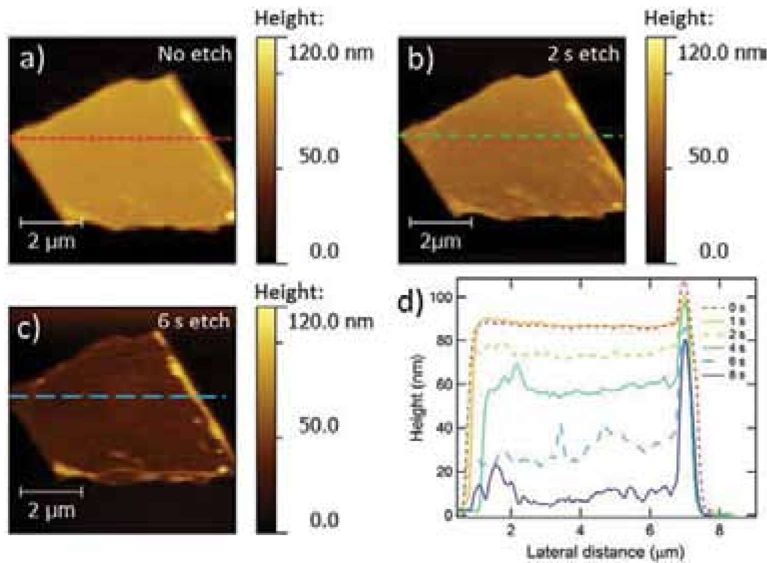

Figure 1. Atomic force microscopy images taken of a Bi_2Se_2 flake (~86 nm thick) before (a) and after 2 s (b) and 6 s (c) of argon plasma etching. The thickness of the flake decreases with continued etching. (d) Measured height profiles along the dashed lines shown in (a–c) for various etching times.

resulting in large disparities in height across the sample after a long plasma etching time. Given enough time (~30 s for this sample), however, even the slowly etched edges of the samples are completely removed from the substrate.

Similar AFM measurements were performed on Bi_2Te_3 (Figure 2), Bi_2Te_2Se (Figure 3) and Sb_2Te_3 after various amounts of plasma etching, with qualitatively similar findings.

Figure 4a shows the average interior thicknesses of four different types of topological insulators – Bi_2Se_3, Bi_2Te_3, Sb_2Te_3 and Bi_2Te_3Se – as functions of plasma etching time. Here the height is averaged over an interior area of the sample to avoid less-etched edges. In our study, we find that the Bi_2Se_3, Bi_2Te_3 and Bi_2Te_2Se samples are all etched at similar rates (~10–13 nm/s), while Sb_2Te_3 has a faster etching rate (~40 nm/s). We also calculate and plot the RMS of the interior heights (Figure 4b), which also indicate an increased surface roughness as etching time increases (except when the sample is almost etched away with height approaching that of the surrounding substrate to cause the RMS to decrease again).

Figure 5a shows the Raman spectra of our Bi_2Se_3 sample before and after exposure to a progression of argon plasma etchings. The initial Raman spectrum shows peaks at 130 cm^{-1} (E_g^2) and 173 cm^{-1} (A_{1g}^2), both of which agree well with the values reported in previous works [5–7]. We can also see the tail of the A_{1g}^1 peak – expected to appear at 72 cm^{-1} – but the full peak is largely truncated by the filter. The positions, intensities and widths of the E_g^2 and A_{1g}^2 peaks, determined using Lorentzian fits to the spectra, are plotted in Figure 5b and c. We observe the positions of the E_g^2 and A_{1g}^2 peaks remain relatively constant throughout the etching

Downloaded by [Purdue University] at 14:10 13 February 2013

Downloaded by [Purdue University] at 14:10 13 February 2013

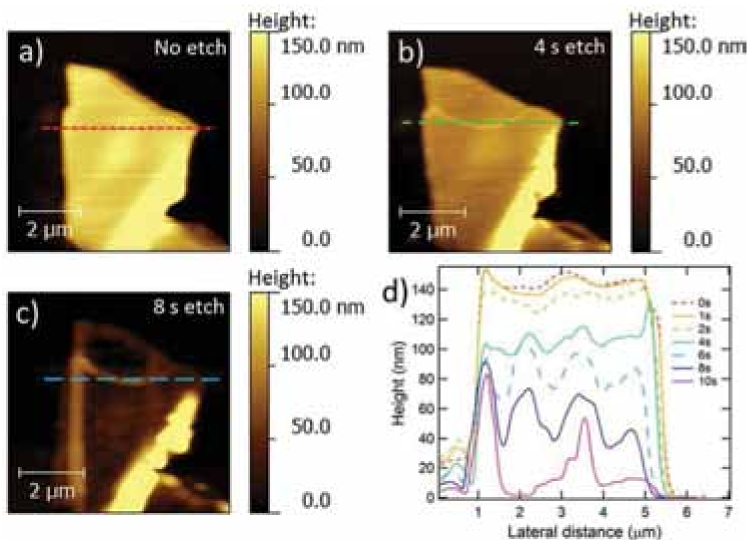

Figure 2. Atomic force microscopy images taken of a Bi_2Te_2 flake (~130 nm thick) before (a) and after 4 s (b) and 8 s (c) of argon plasma etching. The thickness of the flake decreases with continued etching. (d) Measured height profiles along the dashed lines shown in (a–c) for various etching times.

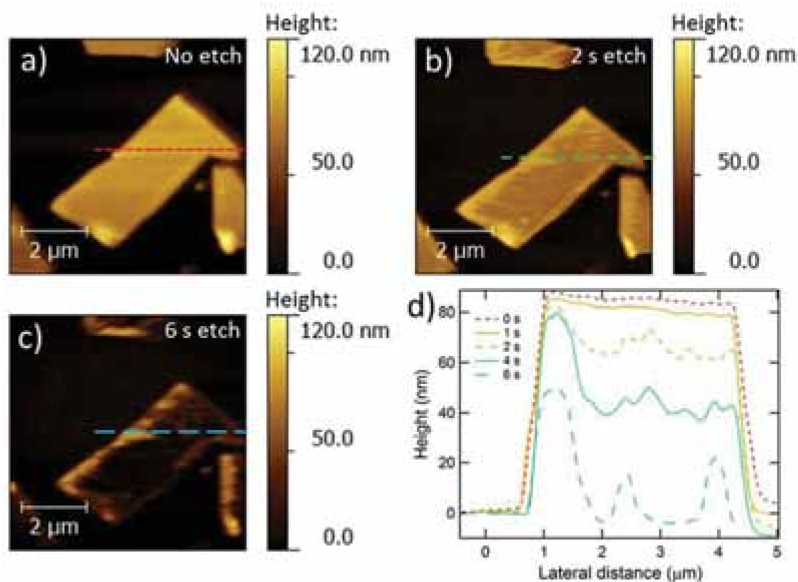

Figure 3. Atomic force microscopy images taken of a Bi_2Te_2Se flake (~94 nm thick) before (a) and after 2 s (b) and 6 s (c) of argon plasma etching. The thickness of the flake decreases with continued etching. (d) Measured height profiles along the dashed lines shown in (a–c) for various etching times.

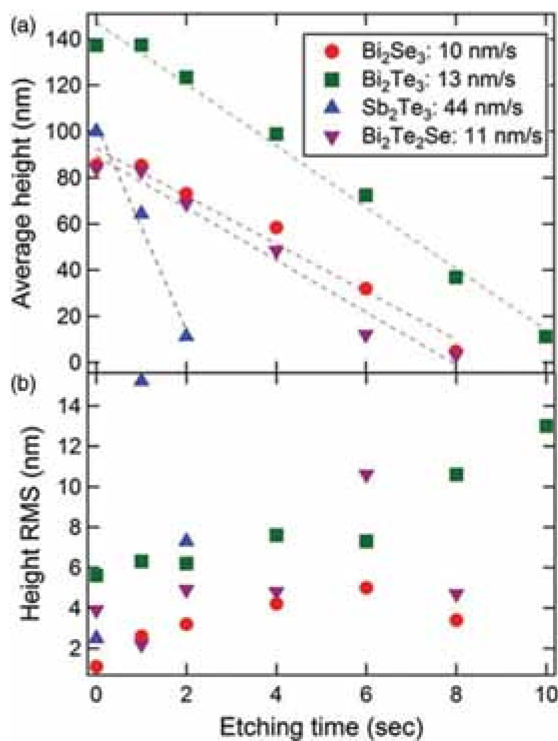

Figure 4. (a) Average sample height versus plasma etching time for four different types of topological insulator samples. Prior to etching, all samples were around 100 nm thick. The height is averaged from an interior area of the sample. The Bi_2Se_3, Bi_2Te_3 and Bi_2Te_2Se samples are all etched at similar rates (~10–13 nm/s), while Sb_2Te_3 has a faster etching rate of ~40 nm/s in this test. (b) The RMS of the interior heights versus plasma etching time. The RMS increases as the etching increases, indicating increased surface roughness.

Downloaded by [Purdue University] at 14:10 13 February 2013

process, as seen in Figure 5b. We do, however, observe a moderate increase in the width of the E_g^2 peak with increased etching time, as also seen in Figure 5b. Figure 5c shows an increase in the intensity of both the E_g^2 and A_{1g}^2 peaks with increased etching before the intensity of the entire spectra decreases sharply as most of the flake is etched away. The intensity ratio $I(E_g^2)/I(A_{1g}^2)$ largely decreases as etching increases, as seen in Figure 5c.

We see similar trends in the progression of the Raman spectra of Bi_2Te_3 (Figure 6) and Bi_2Te_2Se (Figure 7) to those observed in Bi_2Se_3. The initial Raman spectrum of Bi_2Te_3 shows peaks at 100 cm^{-1} (E_g^2) and 132 cm^{-1} (A_{1g}^2), which agree well with values from previous reports [5,8,9], and the initial Raman spectrum of Bi_2Te_2Se shows peaks at 101 cm^{-1} (E_g^2) and 138 cm^{-1} (A_{1g}^2). In the case of Bi_2Te_3, we note both the E_g^2 and A_{1g}^2 peak show a pronounced widening even for relatively small levels of plasma exposure.

We observe an increase in the Raman spectrum intensities of all our studied materials as plasma exposure increases, reaching the highest intensities when our sample thicknesses are reduced to ~20 nm (before the flake is etched away).

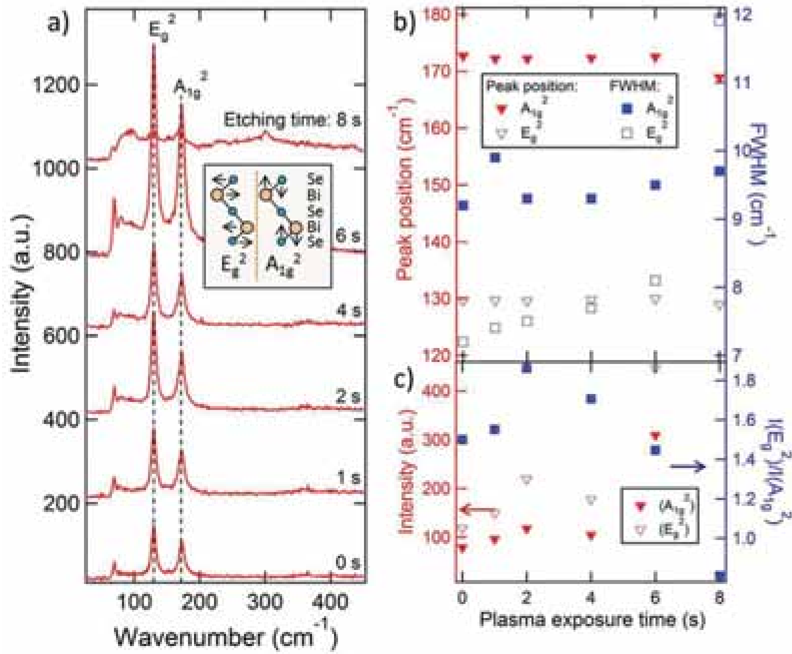

Figure 5. (a) Progression of Raman spectrum of an 86 nm-thick Bi_2Se_3 sample subjected to various amounts of argon plasma etching. The etching time is accumulated over a series of exposures. Spectra are offset vertically for clarity and are measured using a 532 nm excitation laser. The initial Raman spectrum shows peaks at ~130 cm^{-1} and ~173 cm^{-1}, corresponding to the E_g^2 and A_{1g}^2 vibrational modes (inset). (b) The positions and full widths at half max of the E_g^2 and A_{1g}^2 peaks as a function of argon plasma exposure time. (c) The intensity of the E_g^2 and A_{1g}^2 peaks, as well as the intensity ratio $I(E_g^2)/I(A_{1g}^2)$ as a function of argon plasma etching time.

Downloaded by [Purdue University] at 14:10 13 February 2013

Previous reports have also measured an increase in Raman intensity for sufficiently thin films. This intensity increase has been attributed to constructive interference of internal reflections of the Raman signal in the films [6,10–12] We have also seen similar trends in Raman intensities as dependent on the thickness using un-etched TI flakes (see supplemental materials) consistent with those in previous reports. However, for our plasma etched samples, we see increases in intensity at thicknesses larger than those seen in previous reports [6]. We attribute this to increased roughness on the material surface causing areas of the sample reaching thickness lower than the average thickness.

We also note a decreasing trend in the intensity ratio $I(E_g^2)/I(A_{1g}^2)$ (particularly pronounced for Bi_2Te_3) as plasma etching increases. In a previous report, a reduction in this intensity ratio for thinner Bi_2Te_3 films is attributed to the emergence of infrared modes (A_{1u} and A_{2u}, the latter of which has the same frequency as A_{1g}^2) [13]. Infrared modes becoming Raman active is caused by a breaking of inversion symmetry, which has been attributed in thin TI films to be caused by a breaking of crystal symmetry or built-in electric fields on the surface of the material [6,13].

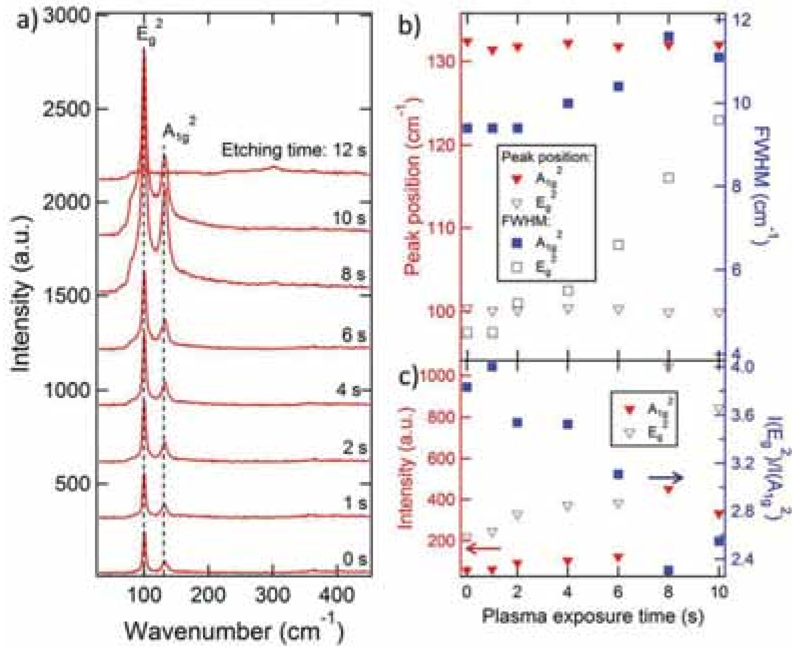

Figure 6. (a) Progression of Raman spectrum of a 130 nm-thick Bi_2Te_3 sample subjected to various amounts of argon plasma etching. The etching time is accumulated over a series of exposures. Spectra are offset vertically for clarity and are measured using a 532 nm excitation laser. The initial Raman spectrum shows peaks at ~100 cm^{-1} and ~132 cm^{-1}, corresponding to the E_g^2 and A_{1g}^2 vibrational modes. (b) The positions and full widths at half max of the E_g^2 and A_{1g}^2 peaks as a function of argon plasma exposure time. (c) The intensity of the E_g^2 and A_{1g}^2 peaks, as well as the intensity ratio $I(E_g^2)/I(A_{1g}^2)$ as a function of argon plasma etching time.

We note, however, in our case we do not see an emergence of the A_{1u} (116 cm^{-1}) IR-activated peak in our plasma-etched samples. This could be related to doping in our samples causing an insufficient E-field on the surface or the defects in our samples.

The other significant trend in Raman spectra we observe is the increasing width of the A_{1g}^2 and E_g^2 peaks as plasma etching increases. Widening of the Raman peaks can be attributed to a decrease in phonon lifetime, caused by increased phonon scattering in the sample [14]. A previous report has noted an increase in Raman peak width in sufficiently thin TI films (<15 nm) [7]. In this study, we see an increased width even for relatively thick films (~80 nm). We suggest that the disorder and surface roughness generated by plasma etching may play an important role in phonon scattering and Raman peak broadening in our samples.

To reinforce the evidence that this increased peak width is largely caused by plasma-induced disorder (rather than just a thickness reduction), we also measured the Raman spectra of pristine peeled Bi_2Se_3 and Bi_2Te_3 films for a wide range of thicknesses (see Figure S1 in the online supplemental information) and saw no significant increase in A_{1g}^2 and E_g^2 peak width down to ~10 nm thickness.

Downloaded by [Purdue University] at 14:10 13 February 2013

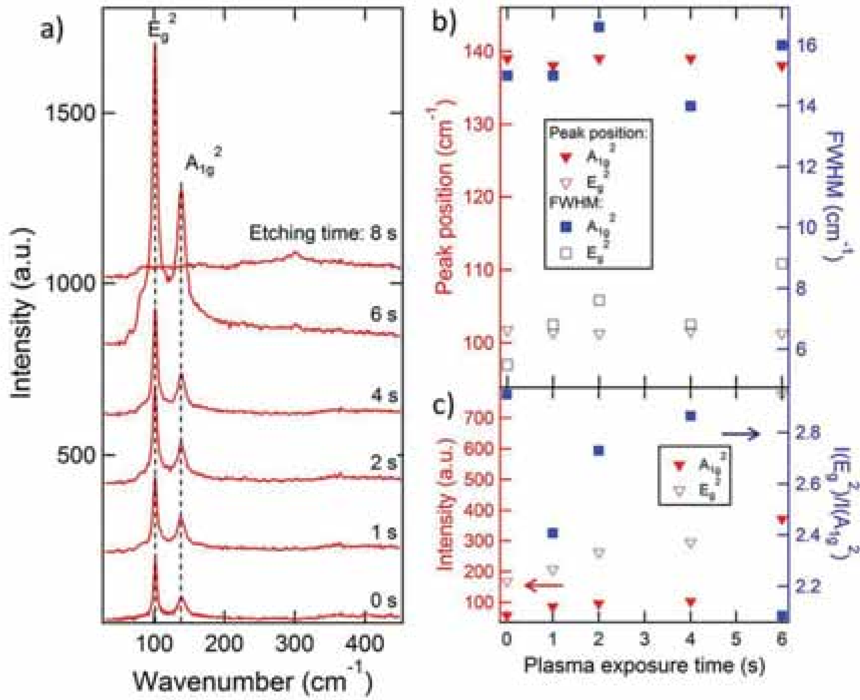

Figure 7. (a) Progression of Raman spectrum of a 94 nm-thick Bi_2Te_2Se sample subjected to various amounts of argon plasma etching. The etching time is accumulated over a series of exposures. Spectra are offset vertically for clarity and are measured using a 532 nm excitation laser. The initial Raman spectrum shows peaks at ~101 cm^{-1} and ~138 cm^{-1}, corresponding to the E_g^2 and A_{1g}^2 vibrational modes. (b) The positions and full widths at half max of the E_g^2 and A_{1g}^2 peaks as a function of argon plasma exposure time. (c) The intensity of the E_g^2 and A_{1g}^2 peaks, as well as the intensity ratio $I(E_g^2)/I(A_{1g}^2)$ as a function of argon plasma etching time.

As an additional indication of the effect of disorder generated by plasma etching, we also measured the magneto-resistance (see Figure S2 online) of a thick (~100 nm) Bi_2Se_3 device before and after a brief amount of oxygen plasma etching that does not significantly reduce the thickness. After the etching, we see emergence of a small weak anti-localization feature, indicating increased electron scattering from defects generated by plasma etching [15]. A more systematic study of the electronic transport properties of plasma-etched TI samples is however beyond the scope of the current work, which focuses on AFM and Raman studies.

4. Conclusions

In summary, we have observed various significant effects due to plasma etching of TI materials. From AFM measurements, we see a decrease in sample thickness and an increase in surface roughness for increased plasma exposure. In our Raman

Downloaded by [Purdue University] at 14:10 13 February 2013

measurements, we observe an increase in overall intensity, a decrease in the intensity ratio $I(E_g^2)/I(A_{1g}^2)$ and an increase in peak widths. We attribute these changes in Raman spectra both to decreased sample thickness and increased phonon scattering caused by argon plasma-generated defects and roughness.

Acknowledgements

This work has been partially supported by the Mesodynamic Architectures program of the Defense Advanced Research Projects Agency. Yong P. Chen also acknowledges support from the Miller Family Endowment.

References

[1] M.Z. Hasan and J.E. Moore, Annu. Rev. Condens. Matter Phys. 2 (2011) p.55.
[2] D. Hsieh, Y. Xia, D. Qian, L. Wray, J.H. Dil, F. Meier, J. Osterwalder, L. Patthey, J.G. Checkelsky and N.P. Ong, Nature 460 (2009) p.1101.
[3] I. Childres, L.A. Jauregui, J. Tian and Y.P. Chen, New J. Phys. 13 (2011) p.025008.
[4] H. Cao, J. Tian, I. Miotkowski, T. Shen, J. Hu, S. Qiao and Y.P. Chen, Phys. Rev. Lett. 108 (2012) p.217803.
[5] W. Richter, H. Kohler and C.R. Becker, Phys. Status Solidi B 84 (1977) p.619.
[6] S.Y.F. Zhao, C. Beekman, L.J. Sandilands, E.J. Beschucky, D. Kwok, N. Lee, A.D. LaForge, S.W. Cheong and K.S. Burch, Appl. Phys. Lett. 98 (2011) p.141911.
[7] J. Zhang, Z. Peng, A. Soni, Y. Xiong, B. Peng, J. Wang, M.S. Dresselhaus and Q. Xiong, Nano Lett. 11 (2011) p.2407.
[8] K.M.F. Shahil, M.Z. Hossain, D. Teweldebrhan and A.A. Balandin, Appl. Phys. Lett. 96 (2010) p.153103.
[9] V. Russo, A. Bailini, M. Zamboni, M. Passoni, C. Conti, C.S. Casari, A. Li Bassi and C.E. Bottani, J. Raman Spectrosc. 39 (2008) p.205.
[10] Y.Y. Wang, Z.H. Ni, Z.X. Shen, H.M. Wang and Y.H. Wu, Appl. Phys. Lett. 92 (2008) p.043121.
[11] D. Yoon, H. Moon, Y.-W. Son, J.S. Choi, B.H. Park, Y.H. Cha, Y.D. Kim and H. Cheong, Phys. Rev. B: Condens. Matter 80 (2009) p.125422.
[12] L.J. Sandilands, J.X. Shen, G.M. Chugunov, S.Y.F. Zhao, S. Ono, Y. Ando and K.S. Burch, Phys. Rev. B: Condens. Matter 82 (2010) p.064503.
[13] K.M.F. Shahil, M.Z. Hossain, V. Goyal and A.A. Balandin, J. Appl. Phys. 111 (2012) p.054305.
[14] B. Di Bartolo, *Optical Interactions in Solids*, Wiley, New York, 1968.
[15] J. Chen, H.J. Qin, F. Yang, J. Liu, T. Guan, F.M. Qu, G.H. Zhang, J.R. Shi, X.C. Xie, C.L. Yang, K.H. Wu, Y.Q. Li and L. Lu, Phys. Rev. Lett. 105 (2010) p.176602.

Downloaded by [Purdue University] at 14:10 13 February 2013